

## Quenching of the Size Effects in Free and Matrix-Embedded Silver Clusters

J. Lermé,<sup>1</sup> B. Palpant,<sup>1</sup> B. Prével,<sup>2</sup> M. Pellarin,<sup>1</sup> M. Treilleux,<sup>2</sup> J. L. Vialle,<sup>1</sup> A. Perez,<sup>2</sup> and M. Broyer<sup>1</sup>

<sup>1</sup>*Laboratoire de Spectrométrie Ionique et Moléculaire, CNRS and Université Lyon I, Bâtiment 205, 43 Boulevard du 11 Novembre 1918, 69622 Villeurbanne Cedex, France*

<sup>2</sup>*Département de Physique des Matériaux, CNRS and Université Lyon I, Bâtiment 203, 43 Boulevard du 11 Novembre 1918, 69622 Villeurbanne Cedex, France*

(Received 24 December 1997)

The surface plasmon energy of silver clusters is investigated in the framework of the time-dependent local density approximation. The results are in good agreement with experimental data on free  $\text{Ag}_N^+$  clusters and on  $\text{Ag}_N$  clusters embedded in solid argon and alumina. The size effects are weak and very sensitive to the matrix, the porosity at the interface, and the cluster charge. It is shown that the core-electron contribution to the metal dielectric function is mainly responsible for the quenching of the size effects in the optical response. [S0031-9007(98)06213-9]

PACS numbers: 36.40.-c, 71.10.-w, 71.45.Gm

The core electrons play a central part in the optical properties of noble metals [1]. Contrary to alkali metals, the collective excitations of the  $s$  electrons are strongly modified by the polarization of the core electrons, especially those belonging to the close fully occupied  $d$  band. The screening of the interaction between valence electrons by the  $d$  electrons results in a shift of the collective excitation frequencies to lower energies relative to the predictions obtained within the jellium model [2] or the classical Drude-Sommerfeld theory. These frequencies are located in a narrow energy range (near UV-visible spectral range) at  $\omega_{\text{vol}} = \omega_p / [\text{Re } \epsilon_d(\omega_{\text{vol}})]^{1/2}$  (volume plasmon),  $\omega_{\text{surf}} = \omega_p / [1 + \text{Re } \epsilon_d(\omega_{\text{surf}})]^{1/2}$  (surface plasmon), and  $\omega_{\text{sph}} = \omega_p / [2 + \text{Re } \epsilon_d(\omega_{\text{sph}})]^{1/2}$  (dipolar Mie resonance of a spherical metal particle).  $\omega_p = [3q^2/4\pi r_s^3 \epsilon_0 m]^{1/2}$  is the free-electron plasma frequency, and  $\epsilon_d(\omega)$  is the core-electron contribution to the complex dielectric function of the metal  $\epsilon(\omega)$ .  $r_s$  is the Wigner-Seitz radius of the bulk metal. A blueshift trend is observed in the case of positively charged silver clusters as the cluster size decreases [3], whereas in alkali clusters the finite-size effects are ruled by the electron spillout beyond the particle radius [4]. This so-called spillout effect lowers the average electron density and leads to a redshift trend instead. As a matter of fact, the electron spillout is also present in noble metal clusters  $M_N$ , but the associated size trend is overcome by the blueshift trend induced by a surface effect related to the core electrons. Close to the surface the  $s$  electrons are incompletely embedded inside the ionic-core background. The consequence is that—due to the localized character of the  $d$ -electron wave functions—the screening is less effective over a layer close to the particle surface. In a phenomenological two-region dielectric model, this feature is taken into account by assuming that the continuous polarizable medium mimicking the screening by the core electrons [characterized by  $\epsilon_d(\omega)$ ] extends only up to  $r = R - d$ , where  $R = r_s N^{1/3}$  is the cluster radius (jellium edge), and  $d$  is the thickness of the layer of reduced polarizability [5–8]. Roughly the blueshift trend stems from the increas-

ing importance of the skin region (to which corresponds the large Mie frequency  $\omega_p/\sqrt{3} > \omega_{\text{sph}}$ ) as the cluster radius decreases. The size evolution of the Mie frequency of free charged clusters is thus the net result of the competition between both opposite trends. The size effects are more difficult to interpret or predict in the case of matrix-embedded clusters. The numerous experiments performed on  $\text{Ag}_N$  clusters have pointed out the sensitivity of the size evolution of the Mie frequency on the surrounding matrix, probably on the experimental technique for elaborating the composite films through the metal/matrix interface effects (surface defects, matrix porosity, ...), and the studied size range [1]. In some cases, for instance in solid Ar [6] and CO [9] matrices, the usually expected linear evolution on a  $1/R$  scale is not observed over the entire size range. Depending on the experiment, a redshift [10], a blueshift [9], or a quasi-size-independent evolution [11] is exhibited.

The purpose of this Letter is to rationalize the various seemingly contradictory and unusual results observed on silver clusters. We report on time-dependent local density approximation (TDLDA) [12] investigation of the optical absorption of free and matrix-embedded spherical silver clusters, as well as new experimental results on alumina-embedded silver clusters. The TDLDA was applied within the context of jellium sphere calculations involving concentric spherically symmetric dielectric media [8]. One (at  $r = R - d$ ) and two (at  $r = R - d$  and  $r = R + d_m$ ) interfaces are involved for free and embedded clusters, respectively. Details about our TDLDA calculations, in particular, the change of the Coulomb interaction in the presence of the dielectric media, will be given in a forthcoming paper. The results clearly show that the various observed size trends may be explained by simple dielectric effects.

Actually the great sensitivity of the size evolution to the experimental conditions is found to be closely related to the steep frequency dependence of  $\epsilon_d(\omega)$  near the Mie frequency, leading to a subtle arbitration between the redshift trend induced by the spillout effect and the blueshift

trend induced by the surface skin of ineffective screening. Prior to presenting the raw TDLDA results, it is advisable to analyze qualitatively how the core-electron dielectric function  $\epsilon_d(\omega)$  is expected to influence the size effects in silver clusters. Both components of  $\epsilon_d(\omega)$  are displayed in Fig. 1.  $\epsilon_d(\omega)$  has been extracted from the experimental complex refractive index of bulk silver [13]. In a first step,  $\text{Im} \epsilon_d(\omega)$  is obtained by subtracting from the total imaginary component  $\text{Im} \epsilon(\omega)$  the free-electron contribution parametrized as a Drude-Sommerfeld formula. In a second step, the real component  $\text{Re} \epsilon_d(\omega)$  is obtained by a Kramers-Kronig analysis. More information about the method, which is closely related to the one reported in Ref. [14] (see also Fig. 3 in Ref. [5]), will be given in a more detailed paper. The Mie frequency in the large-size limit is given by solving the approximate classical equation  $\epsilon(\omega) + 2\epsilon_m(\omega) = 0$ , yielding the result

$$\omega(\infty) = \frac{\omega_p}{\sqrt{2\epsilon_m(\omega_\infty) + \text{Re}[\epsilon_d(\omega_\infty)]}}, \quad (1)$$

where  $\epsilon_m(\omega)$ , which is almost constant in the relevant energy range, is the dielectric function of the transparent surrounding matrix ( $\epsilon_m = 1, \approx 1.75, \approx 3.1$  for vacuum, solid argon, and alumina, respectively). Using the value  $r_s = 3.02$  a.u. for calculating  $\omega_p (\approx 9$  eV), one obtains  $\omega(\infty) \approx 3.41$  eV in vacuum.

Inspection of Fig. 1, in view of Eq. (1), clearly suggests that the location of  $\omega(\infty)$  relative to the maximum ( $\omega_{\text{max}}$ ) of the sharp peak in  $\text{Re} \epsilon_d(\omega)$  (located near the interband threshold 3.85 eV) is the key feature ruling the competition between the blueshift and redshift trends. If  $\omega(\infty) < \omega_{\text{max}}$ , the red(blue)shift induced by the spillover effect (skin region of reduced polarizability) is counterbalanced by the decrease (increase) of the denominator in Eq. (1). The net result will be very sensitive to the slope of the  $\text{Re} \epsilon_d(\omega)$  curve. Conversely, if  $\omega(\infty) > \omega_{\text{max}}$  both finite-size effects, i.e., the redshift and blueshift trends, will

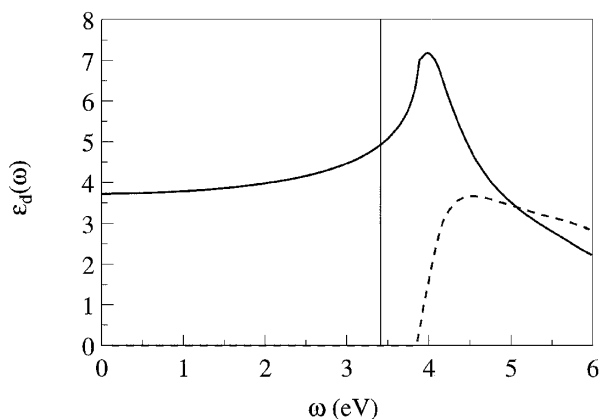


FIG. 1. Spectral dependence of the real (full line curve) and imaginary (dashed line curve) components of the complex dielectric function corresponding to the core electrons for silver metal. The vertical line denotes the Mie frequency for large free clusters.

be magnified. The first case prevails for silver clusters. Namely, any “attempt” for some finite-size effects will be partly quenched by this “locking” phenomenon. The size effects are thus expected to be much smaller in silver clusters than in alkali metals in spite of the lower  $r_s$  value, because of the competition between the opposite trends and the quenching phenomenon induced by the steep frequency dependence of  $\epsilon_d(\omega)$ .

Let us emphasize that, as in previous works, the screening induced by the  $d$  electrons and the embedding matrix are phenomenologically described [7,8]. Hence, only the influence of both polarizable media on the optical response of the  $s$  electrons is investigated in the present model. The real interband transitions which dominate the photoabsorption spectra above 4 eV are therefore not reproduced by our TDLDA calculations. In the latter, a small width has been attributed to the bound-bound transitions of the independent-electron response in order to resolve the (eventual) fragmented pattern of the Mie resonance due to the coupling of the collective mode with the one electron–one hole excitations (Landau damping) [15]. For our study, the size-dependent fragmented pattern of the resonance has been smoothed by convoluting the photoabsorption spectra with a Gaussian curve having a width at half maximum equal to 1 eV. The energy of the resonance maximum is used for the analysis of the mean size effects.

In Fig. 2, the size evolution of the Mie frequency of free closed-electronic shell  $\text{Ag}_N$  clusters is plotted for various values of the thickness parameter  $d$  (black triangles). As expected from the previous qualitative analysis the size effects are weak. A redshift or a blueshift trend is obtained depending on the  $d$  value. For large enough values ( $d > 2$  a.u.), the effect of the skin region of reduced polarizability dominates, but the size evolution does not exhibit a steady linear increase on the  $1/R$  scale. This stems from the increase of the quenching of the blueshift

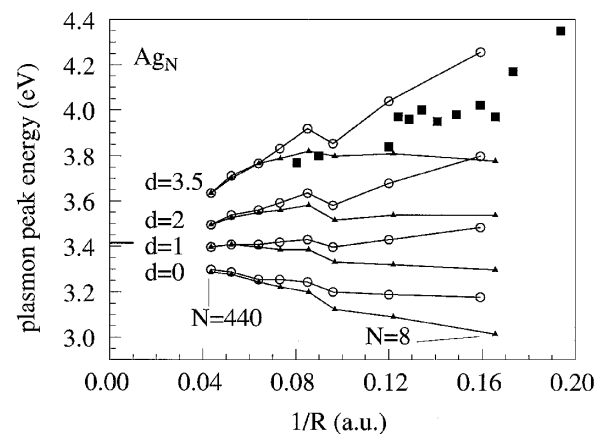


FIG. 2. Size evolution of the maximum of the Mie-resonance peak for free  $\text{Ag}_N$  (triangles) and  $\text{Ag}_N^+$  (circles) clusters within the two-region dielectric model, for different values of the thickness parameter  $d$ . Black squares: experimental data on  $\text{Ag}_N^+$  clusters (Ref. [3]). The short horizontal line at 3.41 eV is the Mie frequency in the large-particle limit.

trend when  $\omega(N) \geq 3.7\text{--}3.8$  eV [large increase of the slope  $d \operatorname{Re} \varepsilon_d(\omega)/d\omega$ ; see Fig. 1]. Experimental data on  $\text{Ag}_N^+$  clusters are indicated by black squares [3]. It is well known that the surface plasmon frequency is shifted to higher (lower) energies for cations (anions) due to the contraction (expansion) of the electron cloud (decrease or increase of the spillout effect, respectively). TDLDA calculations involving positively charged clusters (empty circles in Fig. 2) show that the blueshift is very strong for medium and small clusters, especially for large  $d$  values. From Fig. 2, one can deduce that a thickness parameter  $d$  on the order of 3–3.5 a.u. would bring the theoretical predictions in good agreement with the experimental data. These values are larger, but on the same order of magnitude as those proposed previously in various theoretical approaches [5,7,8], and quite consistent with the microscopical formalism developed by Serra and Rubio [16]. The value  $d = 3.5$  a.u. will be assumed in the following.

The size evolution of the theoretical Mie frequency for  $\text{Ag}_N$  clusters embedded in solid argon is displayed in Fig. 3 (empty squares, lower curve). A perfect metal/matrix interface has been assumed in the model; namely, the continuous medium of dielectric constant  $\varepsilon_m = 1.75$  extends down to the cluster radius  $R$  (fully embedded clusters). Experimental results on neutral  $\text{Ag}_N$  clusters codeposited with the matrix gas on a cooled substrate are indicated by black squares [6,9,17]. The data of Refs. [6,17], joined with a continuous line for guiding the eyes, are mean energies of absorption spectra exhibiting a multipeak pattern, assumed to reflect the splitting of the Mie resonance by ellipsoidal shape deformations. The oscillations are thought by Fedrigo *et al.* [6] to result from the electronic shell structure. Our TDLDA calculations, restricted to spherical magic sizes  $N = 8, 20, 40, \dots$  are not able to reproduce such an oscillating behavior. With regard to the whole set of experimental data one can notice that, as for free

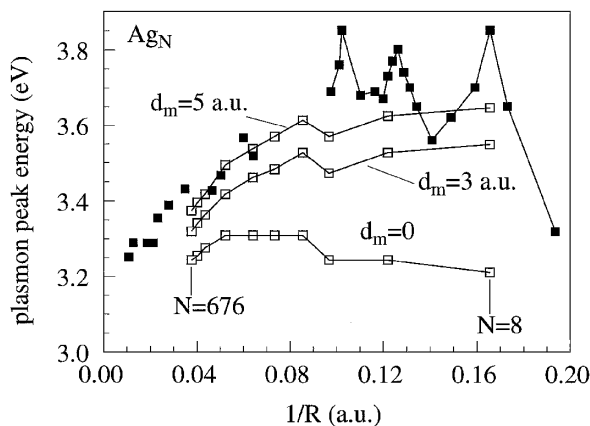


FIG. 3. Size evolution of the maximum of the Mie-resonance peak for  $\text{Ag}_N$  clusters embedded in solid argon within the two-region dielectric model ( $d = 3.5$  a.u.), for different values of the thickness parameter  $d_m$  characterizing the matrix porosity at the interface. Black squares: experimental data of Refs. [9] (large-size range) and [6,17] (small-size range).

neutral clusters in the case of large  $d$  values, the extrapolation of the quasilinear evolution characterizing the large-size domain fails to reproduce the experimental data in the small-size range where the mean evolution is rather flat (oscillation around 3.7 eV). This is a consequence of the energy dependence of the strength of the “quenching effect.” The strong disagreement between the experimental data and the theoretical bell-shaped curve can be rubbed out by taking into account the matrix porosity at the metal/matrix interface. The different chemical nature of the constituents and the surface roughness imply the existence of defects around the cluster, and a large porosity is expected. Hence, a more physically based model would involve a matrix dielectric constant much lower than the bulk value in the vicinity of the cluster surface. The porosity is far from being negligible and is actually a central ingredient for interpreting experimental results on embedded clusters. For instance, characterization of thin films consisting of  $\text{Au}_N$  or  $\text{Ag}_N$  clusters embedded in an alumina matrix elaborated by codeposition on a substrate shows a mean porosity of about 45% [18]. Model calculations involving a perfect “vacuum rind” around the cluster (thickness  $d_m$ ) have been carried out in order to mimic the effects of the local porosity. The results corresponding to the values  $d_m = 3$  and 5 a.u. are displayed in Fig. 3. The experimental mean size evolution is now qualitatively quite well reproduced. Let us emphasize that, for very large  $d_m$  values, the results corresponding to free neutral clusters (see Fig. 2, curve with  $d = 3.5$  a.u.) would be recovered.

Results of TDLDA calculations involving  $\text{Ag}_N$  clusters embedded in an alumina matrix, for various degrees of porosity at the interface, are summarized in Fig. 4 (empty squares). For fully embedded clusters ( $d_m = 0$ ) the size evolution of the Mie frequency exhibits a redshift trend as the cluster size decreases due to the large screening

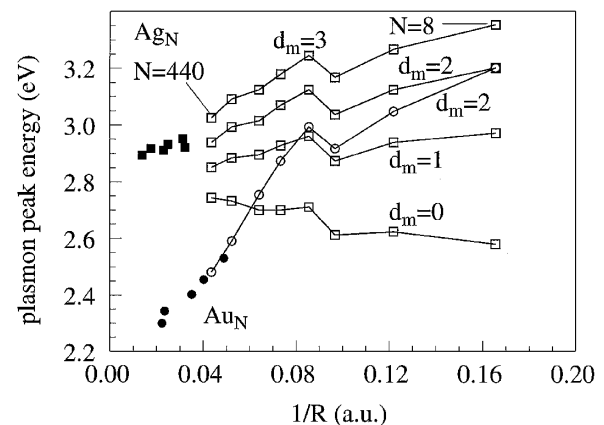


FIG. 4. Size evolution of the maximum of the Mie-resonance peak for  $\text{Ag}_N$  (empty squares) and  $\text{Au}_N$  (empty circles) clusters embedded in alumina within the two-region dielectric model ( $d = 3.5$  a.u.), for different values of the thickness parameter  $d_m$  characterizing the matrix porosity at the interface. The black symbols are the experimental data for silver and gold [18].

of the Coulomb interaction by the matrix polarization (increase of the spillout effect). The trend is inverted when the matrix porosity at the interface is taken into account. This stresses the great sensitivity of the size effects on the characteristics of the interface. The experimental data corresponding to six different particle-size distributions are indicated by black squares (composite films obtained by codeposition on a substrate). The experiments have been carried out under the same experimental deposition conditions as those prevailing for the elaboration of the  $\text{Au}_N:\text{Al}_2\text{O}_3$  thin films [18]. The size effects are almost completely quenched. A slight blueshift trend when the size decreases, consistent with a porosity-parameter  $d_m$  on the order of 2–3 a.u., is, however, visible. Comparison with the optical response of the  $\text{Au}_N:\text{Al}_2\text{O}_3$  samples [18] brings support to our interpretation based on matrix porosity effects at the interface. Calculations involving nonlocal pseudopotentials show that the long range part of the  $nd$ -wave functions are quite similar for Ag and Au atoms. Moreover, both bulk metals have almost identical  $r_s$  values ( $r_s = 3.02$  and  $3.01$  a.u., respectively) [19]. This strongly suggests that the phenomenological parameter  $d$ , as well as  $d_m$ , should be similar for both noble metals. Experimental (black circles) and theoretical (empty circles) results for  $\text{Au}_N$  clusters embedded in alumina are shown in Fig. 4 ( $d = 3.5$  a.u. and  $d_m = 2$  a.u.). The perfect agreement between experiment and theory emphasizes the consistency of our analysis. The much stronger blueshift trend observed with gold metal is a consequence of the  $\omega$  dependence of  $\epsilon_d(\omega)$ . In gold, the interband threshold is lower than in silver ( $\approx 1.9$  eV) and the Mie frequency is close to the peak maximum  $\omega_{\text{max}}$  in the  $\text{Re } \epsilon_d(\omega)$  curve. This leads to a completely different arbitration of the competition between the redshift and blueshift trends, which are quenched and magnified, respectively.

In conclusion, we have shown that the location of the surface plasmon resonance which dominates the optical response of free and matrix-embedded silver clusters is well explained by simple dielectric effects. The matrix porosity at the cluster/matrix interface is of crucial importance for

interpreting the experimental data. The size evolution of the Mie resonance frequency, which is ruled by the competition between the redshift and blueshift trends induced by, respectively, the spillout effect and the surface layer of reduced polarizability, is considerably quenched via the  $\omega$  dependence of the dielectric function corresponding to the fully occupied  $d$  band.

- 
- [1] U. Kreibig and M. Vollmer, *Optical Properties of Metal Clusters* (Springer, New York, 1995).
  - [2] W. Ekaradt, Phys. Rev. B **29**, 1558 (1984).
  - [3] J. Tiggesbäumker, L. Köller, K.H. Meiwes-Broer, and A. Liebsch, Phys. Rev. A **48**, R1749 (1993).
  - [4] W.A. de Heer, Rev. Mod. Phys. **65**, 611 (1993), and references therein.
  - [5] A. Liebsch, Phys. Rev. B **48**, 11 317 (1993).
  - [6] S. Fedrigo, W. Harbich, and J. Buttet, Phys. Rev. B **47**, 10 706 (1993).
  - [7] V.V. Kresin, Phys. Rev. B **51**, 1844 (1995).
  - [8] Ll. Serra and A. Rubio, Z. Phys. D **40**, 262 (1997).
  - [9] K.P. Charlé, W. Schulze, and B. Winter, Z. Phys. D **12**, 471 (1989).
  - [10] M.A. Smithard, Solid State Commun. **13**, 153 (1973).
  - [11] L. Genzel, T.P. Martin, and U. Kreibig, Z. Phys. B **21**, 339 (1975).
  - [12] M.J. Stott and E. Zaremba, Phys. Rev. A **21**, 13 (1980).
  - [13] E.D. Palik, *Handbook of Optical Constants of Solids* (Academic, New York, 1985), Vol. I; *ibid.* (1991), Vol. II.
  - [14] H. Ehrenreich and H.R. Philipp, Phys. Rev. **128**, 1622 (1962).
  - [15] C. Yannouleas and R.A. Broglia, Ann. Phys. (N.Y.) **217**, 105 (1992).
  - [16] Ll. Serra and A. Rubio, Phys. Rev. Lett. **78**, 1428 (1997).
  - [17] W. Harbich, S. Fedrigo, and J. Buttet, Z. Phys. D **26**, 138 (1993).
  - [18] B. Palpant, B. Prével, J. Lermé, E. Cottancin, M. Pellarin, M. Treilleux, A. Perez, J.L. Vialle, and M. Broyer, Phys. Rev. B **57**, 1963 (1998).
  - [19] C. Kittel, *Introduction to Solid State Physics* (Wiley, New York, 1983).